

# Mechanism for carrier velocity saturation in pure organic crystals

V. M. Kenkre

*Department of Physics and Astronomy and Center for Advanced Studies, University of New Mexico, Albuquerque, New Mexico 87131*

P. E. Parris

*Department of Physics, University of Missouri, Rolla, Missouri 65409*

(Received 2 February 2002; published 28 May 2002)

We present a possible mechanism for the saturation of the velocity of photoinjected charge carriers in pure organic crystals, the analysis having been motivated by observations in pentacene. The mechanism is based on the strong wave vector dependence of the damping coefficient appearing in the appropriate effective mass equation. Our primary goal is to explore this mechanism in general terms rather than to apply it to a specific system such as pentacene. Our analysis is based on a Fokker-Planck equation treatment. We indicate how the damping coefficient is related to relaxation times in usual Boltzmann equations and how it can be computed from Fermi golden rule transition rates.

DOI: 10.1103/PhysRevB.65.245106

PACS number(s): 72.10.-d, 72.20.-i, 72.60.+g

## I. INTRODUCTION

Saturation of the velocity of injected charge carriers with increasing electric field has been observed in pure organic crystals such as pentacene.<sup>1</sup> In a recent publication<sup>2</sup> the present authors have analyzed this phenomenon and have shown that, contrary to what has been suggested in the literature,<sup>1,3</sup> drift velocity saturation cannot arise solely as a consequence of the nonparabolic nature of carrier bands. Two possible sources of the saturation have also been sketched in that analysis,<sup>2</sup> one based on the field dependence of the scattering and the other based on its wave vector dependence. Here, we report on specific realizations of the second idea, show what particular features of the quasimomentum dependence can lead to saturation of the velocity, and elucidate the effects of temperature on the phenomenon. Our considerations are based on the standard effective mass equation at zero temperature, augmented into a Langevin form through random noise terms at finite temperatures, and its associated Fokker-Planck equation with quasimomentum-dependent damping.

The effective mass equation for the evolution of the quasimomentum  $\hbar k$  of a carrier valid at zero temperature is

$$\hbar \frac{dk}{dt} + \gamma_k v_k = qE, \quad (1)$$

where  $q$  is the carrier charge,  $E$  is the electric field,  $v_k = (1/\hbar)d\varepsilon_k/dk$  is the group velocity of the carrier obtained from its band energy  $\varepsilon_k$ , and  $\gamma_k$  is the damping coefficient. At finite temperatures, we append a noise term to the right-hand side of Eq. (1) and, through standard procedures, obtain for the evolution of the probability distribution  $f(k,t)$  a Fokker-Planck equation

$$\frac{\partial f(k,t)}{\partial t} = \frac{1}{\hbar^2} \frac{\partial}{\partial k} \left[ \left( \gamma_k \frac{d\varepsilon_k}{dk} - \hbar qE \right) f(k,t) + \gamma_k k_B T \frac{\partial f(k,t)}{\partial k} \right], \quad (2)$$

where  $k_B$  is the Boltzmann constant and  $T$  the temperature. It is important to notice that, unlike in the treatment in the main

body of Ref. 2, but as suggested at the end of that analysis, the damping coefficient  $\gamma_k$  here depends on the location  $k$  of the carrier in the Brillouin zone. Whereas it is clear from the analysis of Ref. 2 that no saturation occurs for a constant  $\gamma$ , the following simple argument shows how a class of  $k$ -dependent damping coefficients result quite naturally in saturation.

## II. ESSENCE OF THE MECHANISM: $T=0$

Consider the zero-temperature case in which the quasi-Newtonian evolution (1) is appropriate. Assume an initial occupation by the carrier of a  $k$  state at or near the center of the Brillouin zone, and take the  $k$  dependence of the damping coefficient to be steep enough so that the carrier, in being accelerated towards the edge of zone, never reaches it and produces no Bloch oscillation, but comes to a steady state where the derivative of  $k$  in Eq. (1) vanishes. The location in the zone at which the carrier lies in the steady state has a  $k$  value which satisfies

$$\gamma_k v_k = qE. \quad (3)$$

The steady-state value of the velocity is  $v_k$  at that value of  $k$ . The field  $E$  that produces this velocity equals  $1/q$  times the value of  $\gamma_k v_k$  at that value of  $k$ . The  $k$  dependence of  $\gamma_k$  will thus be reflected in the field dependence of the velocity. As a result, the plot of  $v$  versus  $E$  will show a saturation if  $\gamma_k$  is sufficiently steep: small changes in  $k$  will result in large changes in  $\gamma_k$  and thereby of  $E$ . In other words, as a consequence of the steepness of  $\gamma_k$ , large changes in the field would be required to produce a discernible change in  $k$  and therefore in the velocity.

The velocity versus field curve is, thus, essentially the  $v_k$  versus  $\gamma_k v_k$  curve. We have shown in Ref. 2 that saturation would occur if  $\gamma_k$  were to have the precise (singular)  $k$  dependence of the effective mass in a band. Such a dependence corresponds, for the case of a sinusoidal band  $\varepsilon_k = -(W/2)\cos ka$ , to the evolution equation

$$\frac{dv}{dt} + \frac{v}{\tau} = \frac{qE}{m^*} = \frac{qEa}{\hbar} \sqrt{v_0^2 - v^2}, \quad (4)$$

where  $a$  is the lattice constant and  $v_0 = Wa$  is the maximum of the group velocity. As explained in Ref. 2, the evolution (4) can be obtained from the effective mass equation (1) by first putting the damping to zero, then dividing by the effective mass  $m^*$ , and finally putting the scattering back in through a term  $-v/\tau$  where  $\tau$  is a constant. Being proportional to the effective mass  $m^*$ , the corresponding  $\gamma_k$  displays a singularity in the middle of the zone: it rises to infinity at  $ka = \pi/2$ , jumps discontinuously to minus infinity, and then rises to a finite negative value at the zone edge.

We would now like to emphasize that the phenomenon of saturation does not require for its explanation such singular, discontinuous, or negative behavior. A steep rise of  $\gamma_k$  in the middle of the zone is all that is necessary. Thus, if  $\gamma_k$  is assumed to have the steepness characteristic of  $m^*$  but not its discontinuity or negative values, e.g., if

$$\gamma_k = \gamma_0 \left[ 1 + \frac{\lambda}{2} \left( \frac{1}{1 + \lambda^2 (ka - \pi/2)^2} + \frac{1}{1 + \lambda^2 (ka + \pi/2)^2} \right) \right], \quad (5)$$

saturation is assured. We display in Fig. 1 the  $k$  dependence of  $\gamma_k$  in the zone and the resulting saturation of the drift velocity with electric field. We assume a sinusoidal band for simplicity and express the velocity and the field in terms of dimensionless quantities  $v/v_0$  and  $E/E_c$  where  $E_c = \gamma_0 v_0 a / q$ . The  $k$  dependence in the damping coefficient (5) has a “resonance shape” because it is derived from the  $k$  dependence of the effective mass (without its discontinuous and negative aspects). All that is necessary for saturation, however, is that  $\gamma_k$  rise steeply enough. An “edge shape” is therefore sufficient. Consider, for instance,

$$\gamma_k = \gamma_0 \{ 2 + \tanh[2(k - k_0)a] - \tanh[2(k + k_0)a] \}, \quad (6)$$

which rises very steeply in the neighborhood of  $k_0$ , as is illustrated in Fig. 2 for three values of  $k_0 = \pi/4, \pi/2$ , and  $3\pi/4$ , along with the consequent occurrence of saturation in the velocity-field plot.

The value of the field  $E$  and the location in the zone where the rise of  $\gamma_k$  is substantial together determine features of the saturation phenomenon. Because the velocity in the band  $v_k$  increases with  $k$  at the center of the zone but reaches a maximum in the middle of the zone (at  $ka = \pi/2$  for a sinusoidal band) and then decreases for larger  $k$  values, a possibility exists that the  $v$ - $E$  plot exhibits a rise followed by a decrease and a saturation at a value smaller than the peak. To illustrate this behavior, we use a tunable damping coefficient

$$\gamma_k = \gamma_0 (1 + \mu \tan^2[k/k_0]), \quad (7)$$

in which the location of the rise can be altered by changing the parameter  $k_0$ . We display in Fig. 3 two curves corresponding to  $k_0 a = 1$  and  $k_0 a = 3/2$ . Saturation occurs at a velocity lower than the maximum in the latter case. While we know of no experiments that display such lower-than-peak saturation, this is an interesting consequence of the mechanism we propose, for systems in which the steep rise in of  $\gamma_k$  occurs far enough from the  $v_k$  peak region.

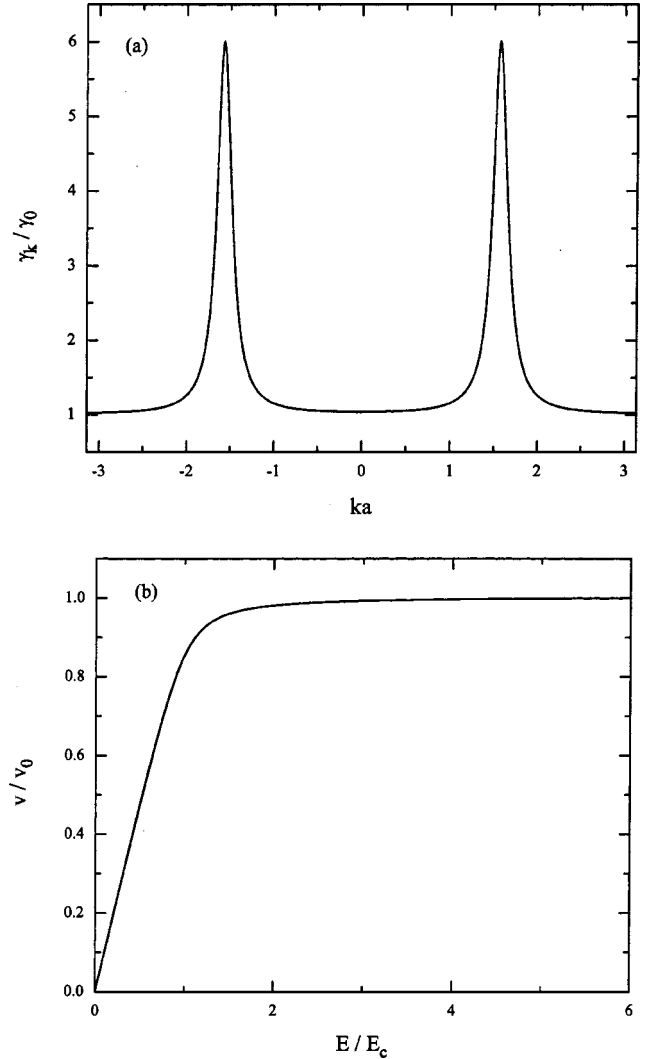


FIG. 1. Saturation of the carrier velocity with increasing field arising from the steep  $k$  dependence of the damping coefficient  $\gamma_k$ . This  $k$  dependence in the Brillouin zone, as given by Eq. (5), is shown in (a) while the corresponding zero-temperature carrier velocity is plotted in (b). Both velocity and field are scaled as explained in the text.

### III. THERMAL EFFECTS ON SATURATION: $T > 0$

We thus see that, while saturation does not arise from the nonparabolic nature of bands, it can arise very simply from steep damping coefficients, at least at zero temperatures. Does finite temperature have any drastic effect on these conclusions? In order to answer this question, we turn to the Fokker-Planck equation (2) which describes the evolution of the distribution function  $f(k, t)$ , i.e., the probability density that the carrier occupies a state  $k$  at time  $t$ . In the steady state,  $f(k, t)$  has a time-independent value (which we will denote below by  $f_k$ ) and the contents of the square brackets on the right-hand side of Eq. (2) equal a  $k$ -independent quantity which may be evaluated in standard ways<sup>6</sup>. Details of this evaluation involve a straightforward extension of our analysis presented earlier<sup>2,4</sup> for the constant  $\gamma$  case. The resulting steady-state distribution  $f_k$  is given by

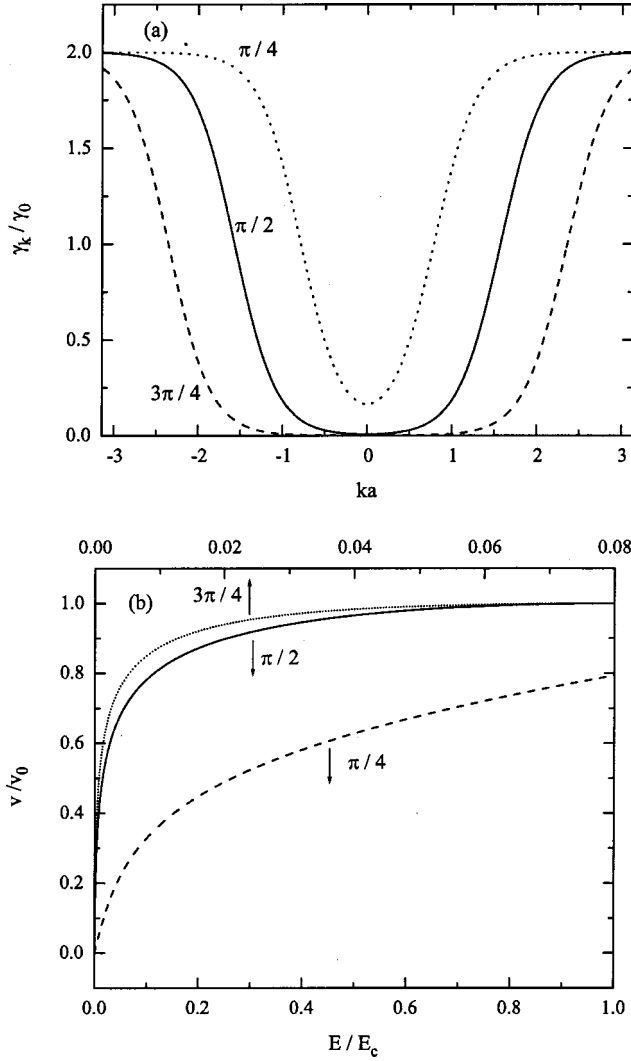


FIG. 2. Saturation as in Fig. 1 but shown here for an “edge”  $k$  dependence as given in Eq. (6). The  $k$  dependence of the damping coefficient is shown in (a) for three values of  $k_0a$ :  $\pi/4$ ,  $\pi/2$ , and  $3\pi/4$ , respectively, which represent different locations in the Brillouin zone where the steep part of  $\gamma_k$  appears. The corresponding zero-temperature velocity-field plot is in (b) where the scale on the upper axis applies to the uppermost curve while that on the lower axis applies to the lower two curves as indicated by arrows.

$$f_k = \frac{\int_0^{2\pi/a} dp h'_{k+p} e^{\beta(\varepsilon_{k+p} - \varepsilon_k)} e^{-\beta\hbar q E (h_{k+p} - h_k)}}{\int_{-\pi/a}^{\pi/a} dk \int_0^{2\pi/a} dp h'_{k+p} e^{\beta(\varepsilon_{k+p} - \varepsilon_k)} e^{-\beta\hbar q E (h_{k+p} - h_k)}}, \quad (8)$$

where  $a$  is the lattice constant,  $\beta$  is the inverse dimensionless temperature  $1/k_B T$ , and

$$h'_k = \frac{dh_k}{dk} = \frac{1}{\gamma_k}. \quad (9)$$

The steady-state velocity is obtained from  $f_k$  in Eq. (8):

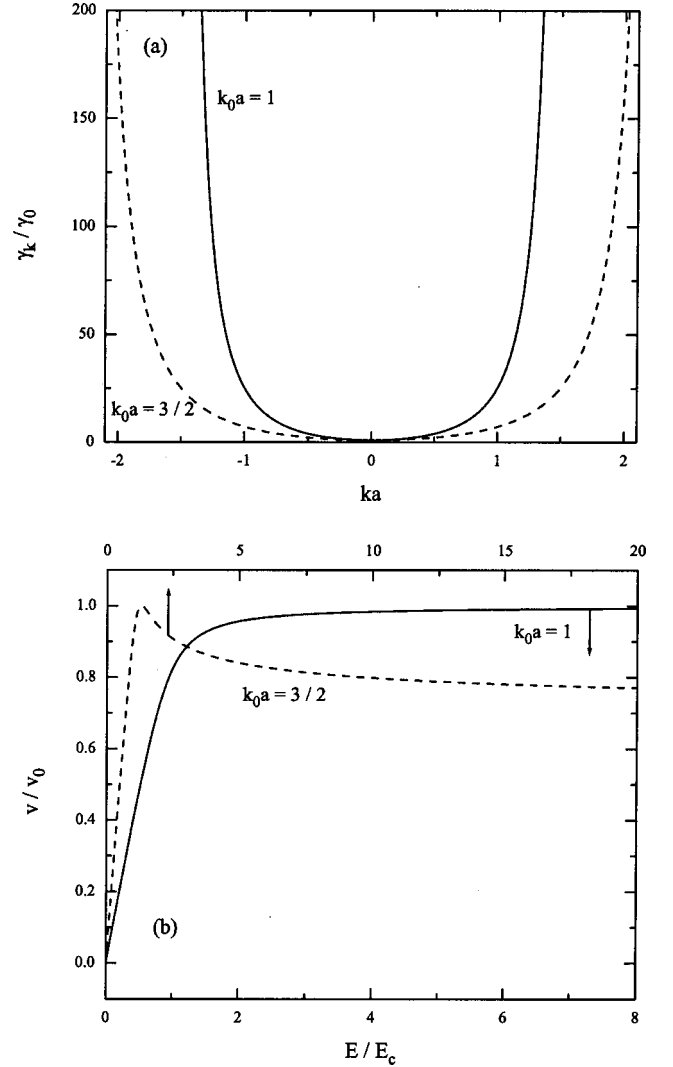


FIG. 3. Saturation below the peak velocity value as the result of the location in the zone of the steep part of  $\gamma_k$ . The  $k$  dependence of the damping coefficient in Eq. (7) is plotted in (a) for values of  $k_0a = 1$  and  $3/2$ , as indicated. The corresponding zero-temperature velocity-field plots in (b) both display saturation, but for  $k_0a = 3/2$  the saturation occurs below the peak value. This is a prediction of our mechanism which, to our knowledge, has not yet been observed.

$$v = \int_{-\pi/a}^{\pi/a} v_k f_k dk. \quad (10)$$

Numerical evaluation procedures allow us to obtain from Eqs. (8) and (10) the distribution and the velocity in the steady state.

In Fig. 4 we display field-dependent velocities for a system with damping coefficient given by Eq. (6) with  $k_0a = \pi/2$ . We notice that for the parameter values considered, saturation, which does occur at  $T=0$ , is destroyed at the finite temperature values shown. This destruction of saturation manifests itself in the well-known phenomenon of negative differential mobility. If, in the steady state, the carrier finds itself distributed in regions of the Brillouin zone in which  $v_k$  is less than the peak value in the zone, there is a

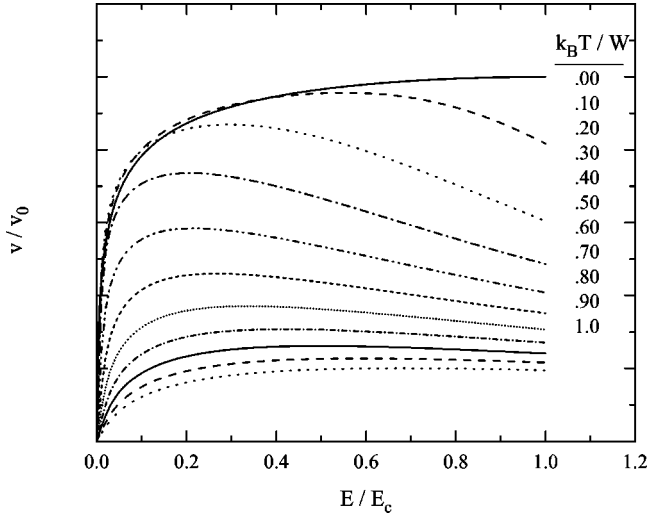


FIG. 4. Effect of nonzero temperature on the saturation phenomenon, showing destruction of saturation and emergence of negative differential mobility. Plotted is the dependence of velocity on field, calculated numerically from the Fokker-Planck equation (2) for a damping coefficient as described by Eq. (6) with  $k_0 a = \pi/2$ , for several different temperatures (scaled to  $W/k_B$ ) as indicated.

tendency for the average velocity to be lowered. Such movement of the carrier into lower-velocity regions occurs as a result of the applied field for constant  $\gamma$  as has been shown in Ref. 2. Here, independently of the action of the field, thermal spreading distributes the carrier in those lower-velocity regions, causing destruction of the saturation.

In order to gain a clearer understanding of these thermal effects, we make use of an analogy between carrier motion in a band and the thermal motion of a classical particle in a potential. Consider the time evolution of the displacement  $x$  of a classical particle of mass  $M$  subjected to a potential  $U(x)$  and to a damping force proportional to the particle velocity  $dx/dt$  through a proportionality factor  $\alpha(x)$  which depends on position

$$M \frac{d^2 x}{dt^2} + \alpha(x) \frac{dx}{dt} + \frac{dU(x)}{dx} = 0. \quad (11)$$

Under very high damping, the inertial term is negligible and we have

$$\frac{dx}{dt} + \frac{1}{\alpha(x)} \frac{dU(x)}{dx} = 0. \quad (12)$$

If we recast the effective mass equation (1) for the injected carrier in the form

$$\frac{dk}{dt} + \frac{\gamma_k}{\hbar^2} \frac{d}{dk} (\varepsilon_k - \hbar q E h_k) = 0, \quad (13)$$

with  $h_k$  given by Eq. (9), and compare Eq. (12) with Eq. (13), we see that the motion of the carrier in the band can be understood intuitively in terms of the motion of the corresponding classical problem.<sup>5</sup> The “potential” to which the carrier is subjected in  $k$  space is  $\varepsilon_k - \hbar q E h_k$ . It has the pe-

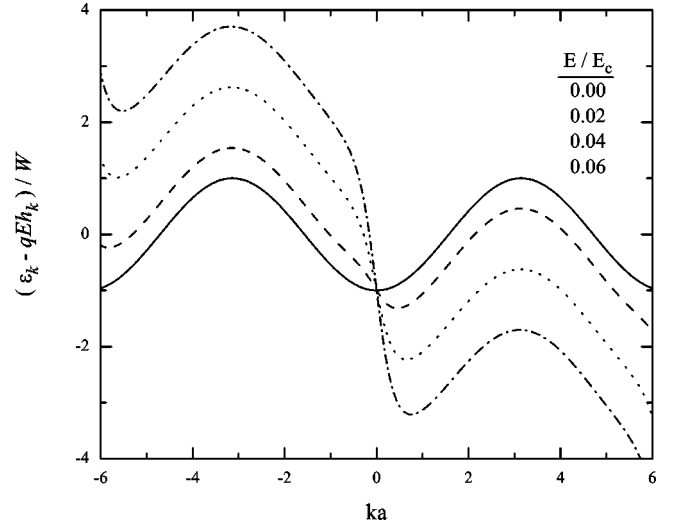


FIG. 5. Field-induced distortion of the effective potential seen by a carrier, showing considerable departure from the sinusoidal band shape. The damping coefficient  $\gamma_k$  is as described by Eq. (6) with  $k_0 a = \pi/2$ . Several different values of the scaled field are shown. The effective potential facilitates, through a classical analogy (see text), the understanding of temperature effects on saturation. The minimum of the potential, located at  $ka=0$  for zero field, moves to the right with increasing field, but due to the strong increase in  $\gamma_k$  with  $k$ , its relative motion slows down, leading to saturation. In this example, the minimum becomes sharper and less shallow as the field is increased, an effect which tends to focus the probability distribution at low temperatures.

riodic dependence characteristic of the band energy, modified by the damping coefficient and the strength of the applied field. If the damping coefficient is not dependent on  $k$ , the potential is  $\varepsilon_k - qE\hbar k/\gamma$  and is, thus, a linearly displaced sinusoid for a tight-binding band. For  $k$ -dependent damping, which is of interest to the present investigation, the steepness characteristics of  $\gamma_k$  are reflected in the potential, and determine the extent of the thermal effects on saturation. In Fig. 5 we plot the effective potential seen by a carrier for a system with damping constant given by Eq. (6) with  $k_0 = \pi/2$ . At  $T=0$ , the carrier settles down at the minimum of the potential. If the location of the minimum (in  $k$  space) has little sensitivity to changes in the field  $E$  as a result of the steepness of  $\gamma_k$  as shown in Sec. II, field saturation of the velocity occurs. As the temperature becomes nonzero, thermal fluctuations tend to move the carrier out of the minimum. Equivalently, the distribution function  $f_k$ , which at  $T=0$  is a  $\delta$  function localized at the potential minimum, spreads in the Brillouin zone because of thermal fluctuations. The velocity  $v$ , which at  $T=0$  is simply the value of  $v_k$  at the potential minimum, now is an average, as in Eq. (10). As the population  $f_k$  grows in regions where  $v_k$  has values lower than the peak, the average velocity decreases, destroying the phenomenon of saturation.

Further quantitative insight may be gained by investigating the dependence of the width as well as the peak of the steady state distribution  $f_k$  on temperature, field strength, and characteristics of  $\gamma_k$ . For this purpose, we focus attention on the primary integral appearing in the steady-state solution (8)

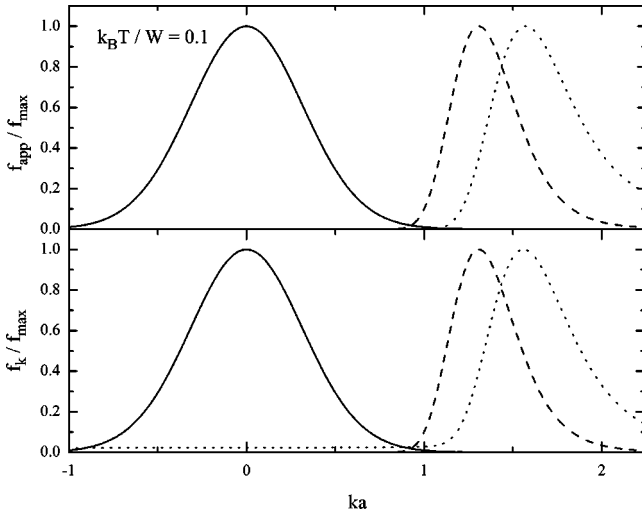


FIG. 6. Comparison of the approximate (top) and actual (bottom) expressions for  $f_k$  as given by Eqs. (15) and (8), respectively, for  $\gamma_k$  given by Eq. (6) with  $k_0 a = \pi/2$ ,  $T = 0.1(W/k_B)$ , and increasing values of the scaled field  $E/E_c = 0, 0.5$ , and  $1$ , respectively, for the solid, dashed, and dotted curves shown. The approximation, which forms the basis of a classical analogy used to understand temperature effects, is seen to be excellent for the parameter values shown.

for the distribution function and, by making a change of integration variable  $k+p \rightarrow p$ , rewrite the integral as a product of two factors:

$$\int_0^{2\pi/a} dp h'_{k+p} e^{\beta(\varepsilon_{k+p} - \varepsilon_k)} e^{-\beta \hbar q E (h_{k+p} - h_k)} \\ = e^{-\beta(\varepsilon_k - \hbar q E h_k)} \int_k^{k+2\pi/a} dp h'_p e^{\beta \varepsilon_p} e^{-\beta \hbar q E h_p}. \quad (14)$$

The second factor on the right-hand side of Eq. (14) is an integral which, being an average over a full Brillouin zone starting at wave vector  $k$ , is a weak function of  $k$ . Under the approximation that its (weak) dependence on  $k$  may be neglected, the distribution function in Eq. (8) is well represented by the simpler expression

$$f_k = \frac{e^{-\beta(\varepsilon_k - \hbar q E h_k)}}{\int_{-\pi}^{\pi} e^{-\beta(\varepsilon_{k'} - \hbar q E h_{k'})} dk'}. \quad (15)$$

Figure 6 compares the distribution as predicted by Eqs. (15) and (8) for a system with damping coefficient given by Eq. (6) to illustrate the validity of the approximation represented by Eq. (15).

For reasonable physical systems, damping rates  $\gamma_k$  are always positive and  $h_k = \int_0^k \gamma_{k'}^{-1} dk'$  is a monotonically in-

creasing function of  $|k|$ . The location  $k_p$  of the peak of  $f_k$ , found by putting the  $k$  derivative of the exponent in the numerator of Eq. (15) to zero, satisfies

$$(\gamma_k v_k)_{k=k_p} = qE, \quad (16)$$

which is precisely equivalent to the condition (3) at zero temperature obtained from the quasi-Newtonian treatment. At low temperatures, as anticipated, the distribution function  $f_k$  approaches a  $\delta$  function centered at the zero-temperature equilibrium value of  $k$ , which marks the minimum of the potential. For finite temperatures, on the other hand, the distribution acquires a width about the peak. The mean velocity, obtained by averaging  $v_k$  over this finite width thus attains a temperature dependence. For the zero-temperature saturation to persist at finite temperatures, the width, of the peak must remain small. Indeed, at high enough temperatures, the spread of the distribution about its zero-temperature value will ultimately cause the velocity to decrease with increasing temperature.

To determine conditions favorable for saturation, we represent  $f_k$  as a Gaussian by expanding the exponent  $\beta(\varepsilon_k - \hbar q E h_k)$  of the distribution function in Eq. (15) up to second order:

$$f_k \approx C e^{-\beta(\varepsilon_{k_p} - \hbar q E h_{k_p})} e^{-(k-k_p)^2/2\sigma^2}, \quad (17)$$

where  $C$  is the normalizing constant. The width  $\sigma$  of the distribution, whose extent is important for the retention or destruction of the saturation phenomenon occurring at  $T = 0$ , is given by

$$\sigma^2 = \frac{m_p^* k_B T}{\hbar + q E m_p^* |h''_{k_p}|}, \quad (18)$$

where  $m_p^*$  is the effective mass  $(1/\hbar^2)(d^2\varepsilon_k/dk^2)$  evaluated at the peak, and  $|h''_k| = (1/\gamma_k^2)(d\gamma_k/dk)$ . Equation (18) shows that the width of the peak in the distribution function increases linearly with the temperature. It also predicts a strong narrowing of the distribution with increasing field provided the rate of change of the inverse damping rates is sufficiently large. Specifically, such narrowing occurs when  $q E m_0^* |h''_{k_p}|/\hbar \gg 1$ , so that the second term in the denominator of Eq. (18) dominates the first, and, additionally, when  $q E |h''_{k_0}| \gg k_B T$ , so that the numerator dominates the denominator. This suggests that saturation will be stronger in systems for which the damping rate “turns on” very suddenly, so that  $d\gamma_k/dk$  becomes large in a region where  $\gamma_k$  itself is fairly small.

As a tunable model system on which these ideas may be tested, we consider a system with a damping rate  $\gamma_k$  such that its reciprocal  $h'_k$  is the piecewise linear function:

$$\gamma_k^{-1} = h'_k = \begin{cases} \gamma_0^{-1} & \text{for } k_1 > |k| > 0, \\ \gamma_0^{-1} [1 - (1 - \eta)(k - k_1)/\Delta k] & \text{for } k_1 + \Delta k > |k| > k_1, \\ \eta \gamma_0^{-1} & \text{for } \pi/a > |k| > k_1 + \Delta k. \end{cases} \quad (19)$$

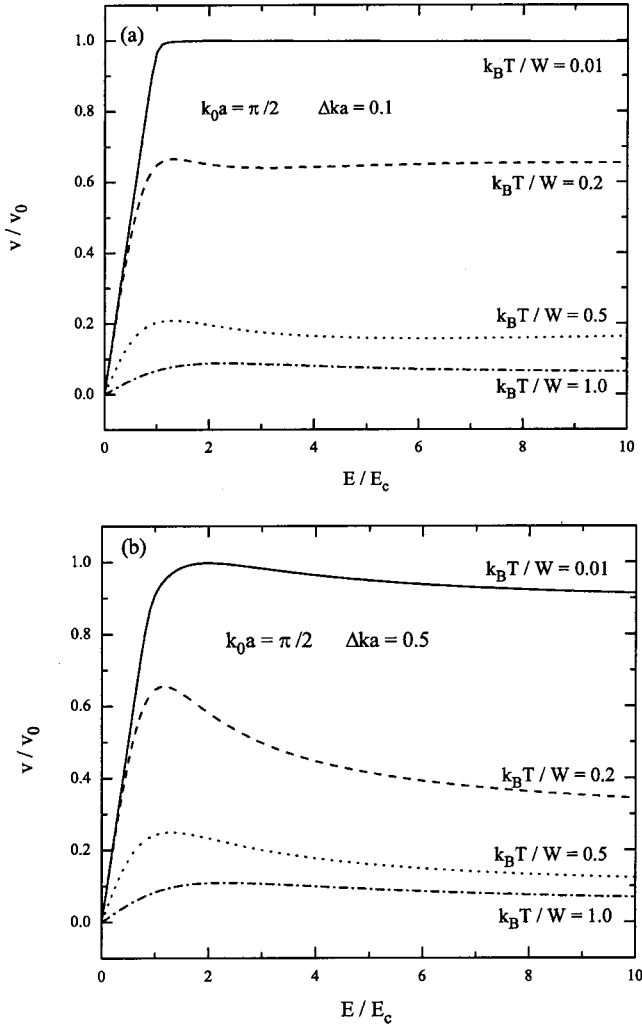


FIG. 7. Numerical calculation of the field-dependent drift velocity from the Fokker-Planck equation (2) for a damping coefficient as described by Eq. (19) with  $k_0 a = \pi/2$  and  $\Delta k a = 0.1$  and  $0.5$ , for several different temperatures as indicated. For all curves the damping coefficient increases by a factor of 100 between  $k = k_0$  and  $k_0 + \Delta k$ . The zero-temperature velocity saturation is more resistant to thermal destruction for small  $\Delta k$ .

The parameter  $\eta < 1$  governs the change that occurs in the inverse damping rate between the zone center and edge, and the crossover interval in the zone where this change occurs extends from  $k_1$  to  $k_1 + \Delta k$ . Choosing  $\eta$  and  $\Delta k$  small maximizes the value of  $h_k''$  in the peak region, since the derivative of Eq. (19) vanishes for  $k$  outside and equals the value  $(1 - \eta)/\Delta k$  inside the crossover interval where the change occurs. Thus, when the peak of the distribution takes a value between  $k_1$  and  $k_1 + \Delta k$ , the width given by Eq. (18) satisfies, for small  $\Delta k$ ,

$$\sigma^2 = \frac{m_0^* k_B T \Delta k}{q E m_0^* (1 - \eta)}. \quad (20)$$

Variation of the parameter  $\Delta k$  controls the width and therefore the persistence or destruction of the saturation phenomenon. In Fig. 7 we present numerical calculations of the

field-dependent drift velocity from the Fokker-Planck equation (2) for a damping coefficient as described by Eq. (19) with  $k_0 a = \pi/2$  and  $\Delta k a = 0.1$  and  $0.5$ , for several different temperatures as indicated. For all curves shown,  $\eta = 0.01$ , so that the damping coefficient increases by a factor of 100 between  $k = k_0$  and  $k_0 + \Delta k$ . We note that, as predicted, the velocity saturation observed at zero temperature is more resistant to thermal destruction when  $\Delta k$  is small.

#### IV. PRESCRIPTION TO COMPUTE $\gamma_k$ AND CONCLUSIONS

The foregoing analysis has provided a possible mechanism, by no means unique, for the saturation of injected carrier velocity with increasing electric field in pure organic crystals. The basis is merely an appropriate  $k$  dependence of damping coefficients. In light of our previous discussion<sup>2</sup> of the earlier arguments of Warta and Karl,<sup>3</sup> one might be tempted to explain the observed velocity saturation in pentacene with the assumption that the source of the scattering is the spontaneous emission of optical phonons. Such scattering is indeed ineffective until the carrier energy exceeds that of the phonons emitted, and thus would suddenly “turn on” at a finite value of the electron wave vector. However, quantitative considerations disqualify this explanation in the case of pentacene, in which velocity saturation appears to occur at room temperature. Optical phonons in pentacene have frequencies of the order of 8–25 meV, which are thus easily absorbed and emitted at room temperature ( $kT \sim 25$  meV). A sudden turn-on of the scattering rate would thus not be expected to occur. One must look to sources other than Shockley’s<sup>8</sup> to bring about the mechanism we have discussed. The specification of the sources of mechanism lies beyond the scope of the present study which primarily indicates constraints on microscopic scattering mechanisms that are required by the observed velocity saturation.

The investigation in the present paper has proceeded under the working assumption that the observed saturation is a real phenomenon. There is another intriguing possibility, recently suggested by Conwell and Basko,<sup>9</sup> that the saturation may be an artifact arising from an interpretation of current-voltage curves on the basis of a formula that inappropriately assumes a field-independent mobility. The explanation of saturation proposed in Ref. 9 requires the existence of a regime of negative differential mobility of the type predicted by our earlier analysis.<sup>2</sup> It is, however, completely different in spirit from the explanation proposed in the present paper. We hope that further work will be soon carried out to determine which (if either) of the mechanisms is applicable to experiments in pentacene.

It is important not to confuse  $\gamma_k$  with the inverse of the more familiar relaxation time  $\tau_k$  which appears in standard Boltzmann equation treatments<sup>7</sup> of carrier transport in materials. We have pointed out in our earlier analysis<sup>2</sup> that identification of critical fields predicted by two separate theories, one based on a Boltzmann equation treatment with a constant relaxation time  $\tau$  and the other based on a Fokker-Planck equation treatment with a constant rate  $\gamma$ , yields

$$\gamma = \frac{\hbar}{\tau a v_0} = \frac{m_0^*}{\tau}. \quad (21)$$

This means that  $\gamma$  is  $1/\tau$  times the minimum value of the effective mass (at the zone edge). However, the relationship between the two quantities in the general  $k$ -dependent case appears not to be known. We present the following connection starting from a master equation

$$\frac{df(k,t)}{dt} = \sum_{k'} [Q_{kk'} f(k',t) - Q_{k'k} f(k,t)], \quad (22)$$

which, under two different respective approximations, results in the Fokker-Planck equation (2) involving  $\gamma_k$ , and the Boltzmann equation under the relaxation time ansatz involving  $\tau_k$ . With the notation  $Q_{kk'} = Q(k', k - k')$ , we can write

$$\begin{aligned} Q_{kk'} f(k',t) &= Q(k+q, -q) f(k+q,t) \\ &\approx \left( 1 + q \frac{\partial}{\partial k} + \frac{q^2}{2} \frac{\partial^2}{\partial k^2} \right) [Q(k, -q) f(k,t)] \end{aligned} \quad (23)$$

by stopping the Taylor expansion at second order if the rates decay quickly with increase in  $q = k' - k$ . Substitution in Eq. (22) and a sum over  $k'$ , which is the same as a sum over  $q$ , yields

$$\begin{aligned} \sum_{k'} [Q_{kk'} f_{k'}(t) - Q_{k'k} f_k(t)] \\ &= \frac{\partial f(k,t)}{\partial t} \\ &= - \frac{\partial}{\partial k} [F_k f_k(t)] + \frac{\partial^2}{\partial k^2} [S_k f_k(t)]. \end{aligned} \quad (24)$$

Here  $F_k = \sum_{k'} (k' - k) Q_{k'k}$  is the first moment of the transition rates while  $S_k = \sum_{k'} [(k' - k)^2 / 2] Q_{k'k}$  is the second moment. An additional relation

$$F_k - \frac{dS_k}{dk} = - \frac{S_k}{\hbar^2 k_B T} \frac{d\epsilon_k}{dk} \quad (25)$$

between the moments of the transition rates and the band energy of the carrier follows from detailed balance. Rewriting Eq. (24) in the form (2), we obtain

$$\gamma_k = \frac{\hbar^2}{2k_B T} \sum_{k'} (k - k')^2 Q_{k'k}. \quad (26)$$

On the other hand, the well-known relaxation time approximation, when applied to Eq. (22) in its simplest version, yields

$$\tau_k = \frac{1}{\sum_{k'} Q_{k'k}}. \quad (27)$$

The conjunction of Eqs. (26) and (27) specifies a relationship between  $\tau_k$  of the Boltzmann equation approach and the  $\gamma_k$  of the Fokker-Planck approach.<sup>10</sup>

Transition rates  $Q_{k'k}$  are typically calculated using Fermi's golden rule as applied to the interaction of the carrier with scattering agents such as phonons or defects. Through Eq. (26) we have provided a usable prescription<sup>11</sup> for calculating the damping coefficient  $\gamma_k$  of the Fokker-Planck equation from the transition rates of the master equation. In a subsequent publication we plan to address connections between Fokker-Planck and Boltzmann approaches to practical transport theory.

## ACKNOWLEDGMENTS

We thank Luca Giuggioli for discussions and acknowledge the partial support of this work by the National Science Foundation under Grant Nos. DMR-0097204 and DMR-0097210.

<sup>1</sup>Jan Hendrik Schön, Christian Kloc, and Bertram Batlogg, Phys. Rev. Lett. **86**, 3843 (2001); J. Schön, Ch. Kloc, and B. Batlogg, Phys. Rev. B **63**, 245201 (2001).

<sup>2</sup>V. M. Kenkre and P. E. Parris, Phys. Rev. B **65**, 205104 (2002).

<sup>3</sup>W. Warta and N. Karl, Phys. Rev. B **32**, 1172 (1985).

<sup>4</sup>P. E. Parris, M. Kuś, and V. M. Kenkre, Phys. Lett. A **289**, 188 (2001).

<sup>5</sup>Although  $\gamma_k$  is a measure of the damping in the effective mass equation (1), the role of the classical damping factor  $\alpha(x)$  of Eq. (12) is played by its *reciprocal*, specifically by  $\hbar^2 / \gamma_k$ . This reversal in the interpretation of  $\gamma_k$  arises from the formal analogy of the  $k$  evolution. Physically,  $\hbar k$  is the (quasi)momentum. In the analogy, it plays the role of the classical displacement viewed in the extreme damping limit.

<sup>6</sup>See, e.g., L. E. Reichl, *A Modern Course in Statistical Physics*, 2nd ed. (Wiley, New York 1998); K. Lindenberg and B. J. West, *The Nonequilibrium Statistical Mechanics of Open and Closed Systems* (Wiley, New York, 1990).

<sup>7</sup>See, e.g., J. M. Ziman, *Electrons and Phonons* (Oxford Univer-

sity Press, New York, 1960); M. Dresden, Rev. Mod. Phys. **33**, 265 (1961).

<sup>8</sup>W. Shockley, Bell Syst. Tech. J. **30**, 990 (1951).

<sup>9</sup>E. M. Conwell and D. M. Basko (unpublished). The authors are grateful to E.M. Conwell for making their work available to them prior to publication.

<sup>10</sup>While Eqs. (26) and (27) exhibit the same dimensional relationship between  $\gamma_k$  and  $\tau_k$  as given by Eq. (21), Eq. (26) connects  $\gamma_k$  directly to microscopic transition rates and the temperature.

<sup>11</sup>The prescription (26) requires that the transition rates in the master equation be of sufficiently short range since it assumes a smooth  $k$  variation of  $Q(k,q)f(k)$ . Such an assumption must break down at low temperatures when both  $Q(k,q)$  and  $f(k)$  tend to vary strongly in the neighborhood of  $k=0$ . This breakdown manifests itself in a divergence of the damping rate (26) at low temperatures. As  $T \rightarrow 0$ , it is expected that  $\gamma_k$  at  $T=0$  is a finite quantity. This can be demonstrated explicitly for specific mechanisms directly from  $Q(k,q)$ .